



Article

# Development of an Inflammation-Triggered In Vitro “Leaky Gut” Model Using Caco-2/HT29-MTX-E12 Combined with Macrophage-like THP-1 Cells or Primary Human-Derived Macrophages

Nguyen Phan Khoi Le <sup>1</sup>, Markus Jörg Altenburger <sup>2</sup> and Evelyn Lamy <sup>1,\*</sup>

<sup>1</sup> Molecular Preventive Medicine, University Medical Center and Faculty of Medicine, University of Freiburg, 79108 Freiburg, Germany; phan.khoi.nguyen.le@uniklinik-freiburg.de

<sup>2</sup> Department of Operative Dentistry and Periodontology, University Medical Center and Faculty of Medicine, University of Freiburg, 79108 Freiburg, Germany; markus.altenburger@uniklinik-freiburg.de

\* Correspondence: evelyn.lamy@uniklinik-freiburg.de; Tel.: +49-761-270-82150

**Abstract:** The “leaky gut” syndrome describes a damaged (leaky) intestinal mucosa and is considered a serious contributor to numerous chronic diseases. Chronic inflammatory bowel diseases (IBD) are particularly associated with the “leaky gut” syndrome, but also allergies, autoimmune diseases or neurological disorders. We developed a complex in vitro inflammation-triggered triple-culture model using 21-day-differentiated human intestinal Caco-2 epithelial cells and HT29-MTX-E12 mucus-producing goblet cells (90:10 ratio) in close contact with differentiated human macrophage-like THP-1 cells or primary monocyte-derived macrophages from human peripheral blood. Upon an inflammatory stimulus, the characteristics of a “leaky gut” became evident: a significant loss of intestinal cell integrity in terms of decreased transepithelial/transendothelial electrical resistance (TEER), as well as a loss of tight junction proteins. The cell permeability for FITC-dextran 4 kDa was then increased, and key pro-inflammatory cytokines, including TNF-alpha and IL-6, were substantially released. Whereas in the M1 macrophage-like THP-1 co-culture model, we could not detect the release of IL-23, which plays a crucial regulatory role in IBD, this cytokine was clearly detected when using primary human M1 macrophages instead. In conclusion, we provide an advanced human in vitro model that could be useful for screening and evaluating therapeutic drugs for IBD treatment, including potential IL-23 inhibitors.

**Keywords:** leaky gut; inflammatory bowel disease (IBD); triple-culture; Caco-2; HT29-MTX-E12; THP-1; monocyte-derived macrophage; inflammation; TEER; FITC-dextran 4 kDa (FD4); pro-inflammatory cytokines



**Citation:** Le, N.P.K.; Altenburger, M.J.; Lamy, E. Development of an Inflammation-Triggered In Vitro “Leaky Gut” Model Using Caco-2/HT29-MTX-E12 Combined with Macrophage-like THP-1 Cells or Primary Human-Derived Macrophages. *Int. J. Mol. Sci.* **2023**, *24*, 7427. <https://doi.org/10.3390/ijms24087427>

Academic Editor: Susanne M. Krug

Received: 24 March 2023

Revised: 12 April 2023

Accepted: 15 April 2023

Published: 18 April 2023



**Copyright:** © 2023 by the authors. Licensee MDPI, Basel, Switzerland. This article is an open access article distributed under the terms and conditions of the Creative Commons Attribution (CC BY) license (<https://creativecommons.org/licenses/by/4.0/>).

## 1. Introduction

The “leaky gut”, also known as increased intestinal permeability, describes a damaged (leaky) intestinal barrier caused by the loose tight junctions of intestinal epithelial cell walls. This phenomenon results in the passage of harmful substances such as pathogens and toxic digestive metabolites from the gut into the bloodstream, and then consequently causes systemic inflammation and immune system activation. An increased intestinal permeability has been considered to play an important role in the development and progression of numerous chronic diseases [1–3]. Autoimmune diseases [4,5], food sensitivities and allergies [6,7], asthma [8], neurological conditions [9–11], autism spectrum disorder [12,13], and gut-related disorders like chronic inflammatory bowel disease (IBD) [14–16] have been reported in association with a “leaky gut”. IBD is an umbrella term that is used mainly to describe two chronic inflammatory conditions of the gastrointestinal (GI) tract: ulcerative colitis (UC) and Crohn’s disease (CD). In 2017, about seven million people were suffering

from IBD worldwide [17], with the prevalence surpassing 0.3% of the general population in North America, Oceania, and many European countries. Moreover, IBD has become a global disease in the twenty-first century with rising incidence and prevalence in many regions, particularly in the emerging economies of South America, Eastern Europe, Asia, and Africa [18]. As there is currently no specific cause and cure for IBD, it presents a tremendous financial burden globally due to the substantial direct costs of medical care and the indirect costs related to disability and missed work [19].

To better understand underlying mechanisms and ultimately identify effective treatment options, many researchers have established various cell-based in vitro models of IBD. For decades, the Caco-2 cell line, a heterogeneous human epithelial colorectal adenocarcinoma cell line, has undoubtedly become the most widely accepted in vitro cell model to study the intestinal absorption of drugs, cell membrane permeability, and inflammatory response [20–26]. When growing as a confluent monolayer on inserts, Caco-2 cells differentiate and demonstrate morphological and functional characteristics of small intestinal absorptive cells such as tight junctions, and a brush border with well-developed microvilli on the apical surface [27]. Furthermore, Caco-2 cells also express typical enzymes of normal small-intestinal villus cells, such as disaccharidases and peptidases [28].

On the other hand, this single-cell Caco-2 model has been criticized by many authors, because it lacks mucus production. Based on the Caco-2 cell model, many modifications and improvements have followed [29]. One of the most important enhancements was combining it with the mucin-secreting HT29-MTX-E12 goblet cell line [30]. The proportion of goblet cells among epithelial cell types ranges from 10% in the small intestine to 24% in the distal colon [31]. Therefore, the Caco-2/HT29-MTX-E12 co-culture model then better resembled the human small intestine. In the in vitro system, the presence of mucus can act as an interactive barrier, limiting the free diffusion of small compounds to the cells, and thus helping to avoid overestimation of the permeability of such compounds [32]. Moreover, an increasing number of studies reported that the disruption of bidirectional communication between the intestinal mucus barrier and gut microbiota plays a critical role in the development and progression of several inflammatory conditions such as IBD [33,34].

In IBD, intestinal macrophages become activated, and contribute to chronic intestinal inflammation [35–37]. Intestinal macrophages in the subepithelial lamina propria (LP) are the most abundant mononuclear phagocytes in the body and play a critical role in maintaining intestinal homeostasis. Thus, some researchers have started to combine intestinal cell lines with human macrophage-like cells (e.g., differentiated monocytic THP-1 cells), or monocyte-derived macrophages from peripheral blood mononuclear cells (PBMCs) [38–40]. However, each of these IBD models has its disadvantages, because of either (1) the lack of mucus-producing cells [41–44], (2) a spatial distance between the intestinal cells and macrophages [45–47], or (3) being specifically adapted for buoyant particles [48].

In this study, we developed a complex in vitro triple-culture model of the human intestine, consisting of differentiated human intestinal Caco-2 cells, HT29-MTX-E12 mucin-producing goblet cells (90:10 ratio), cultured on inserts in close contact with either differentiated human macrophage-like THP-1 cells, or primary human monocyte-derived macrophages obtained from PBMCs of healthy donors. The combination of human cell line-derived intestinal cells and macrophages provides a more biological and physiological representation of the complex interactions between the intestinal epithelium and the immune system in health and IBD.

## 2. Results

### 2.1. Establishment of an Inflammation-Triggered, Triple-Culture In Vitro “Leaky Gut” Model Using Caco-2/HT29-MTX-E12 Co-Culture and Macrophage-like THP-1 Cells

A graphic description of the cell culture and the setup of the inflammation-triggered, triple-culture in vitro “leaky gut” model is demonstrated in Figure 1.

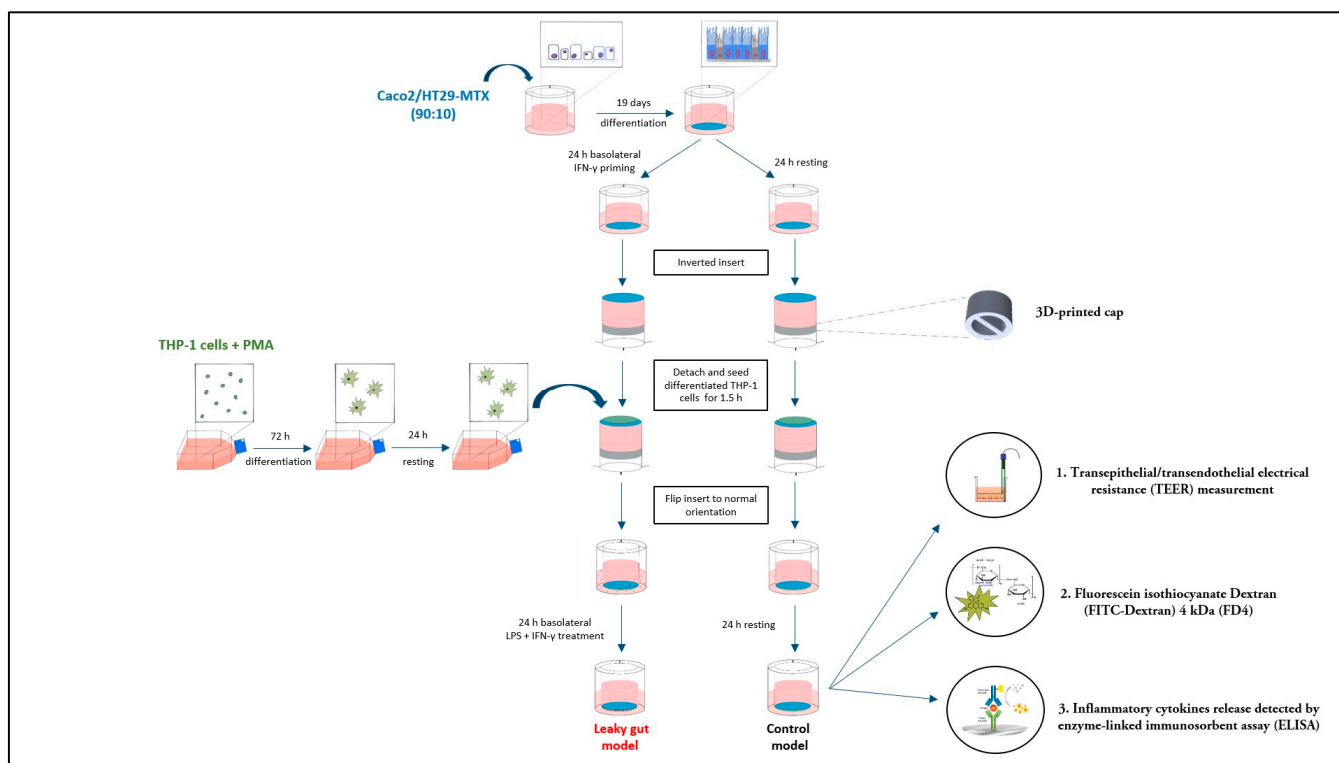


**Figure 1.** Schematic diagram of the inflammation-triggered, triple-culture in vitro “leaky gut” model. 19-day-differentiated Caco-2/HT29-MTX-E12 co-cultures were either rested in fresh medium (control), or primed for 24 h with IFN- $\gamma$ . On the following day, a custom-designed three dimension (3D)-printed cap was carefully placed into the insert of the cultures to confine the medium, before placing the insert upside down in a Petri dish. After that, phorbol 12-myristate 13-acetate (PMA)-differentiated macrophage-like THP-1 cells, or primary monocyte-derived macrophages were transferred on the bottom side of the inverted inserts for 1.5 h, before flipping it back to the regular orientation. Then, for generating the inflammation-mediated “leaky gut” condition, macrophages were activated for 24 h by adding a combination of LPS and IFN- $\gamma$ . At the same time, for the control model, macrophages were rested in medium for this time.

## 2.2. Custom-Designed Three Dimension (3D)-Printed Cap for Medium Confinement in the Insert

A cap was 3D designed (Figure 2A–C) to fit into the insert and sealed the setup by friction. The base of the cap was shaped conically to eliminate possible air pockets when the cap was inserted into the insert (Figure 2D,E).

## 2.3. Characterization of 21-Day-Differentiated Caco-2/HT29-MTX-E12 (90:10 Ratio) Co-Culture

The development of cell monolayer integrity of the Caco-2/HT29-MTX-E12 co-culture during the 21-day incubation was determined by transepithelial/transendothelial electrical resistance (TEER) measurement, which is a widely accepted quantitative technique to assess the integrity of cellular barriers in cell culture models [49]. As presented in Figure 3A, the TEER value of HT29-MTX-E12 cells increased from  $18 \pm 9 \Omega \cdot \text{cm}^2$  to  $128 \pm 18 \Omega \cdot \text{cm}^2$  between day 3 to 21 of cultivation. In contrast, the TEER values of the Caco-2 monoculture, and the Caco-2/HT29-MTX-E12 co-culture reached  $660 \pm 31 \Omega \cdot \text{cm}^2$  and  $605 \pm 29 \Omega \cdot \text{cm}^2$  on day 21, respectively. Therefore, in this study, only co-cultures of Caco-2/HT29-MTX-E12 with TEER values above  $300 \Omega \cdot \text{cm}^2$  were used in further experiments.

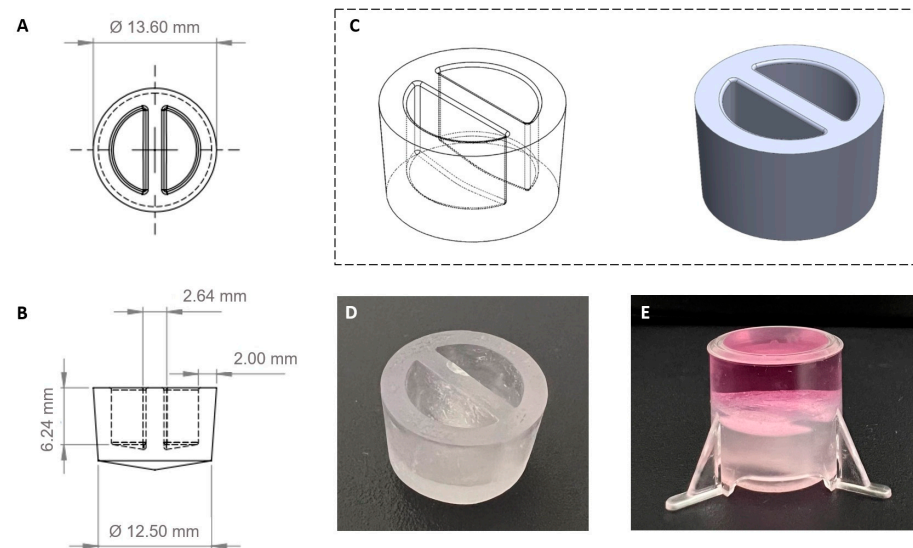


**Figure 2.** Custom-designed 3D-printed cap. The design sketches of the cap are: top view (A), front view (B), and 3D view (C). The dimensions of this cap (D) were determined to fit into the insert perfectly to safely confine the medium within the insert during the macrophage adherence procedure (E).

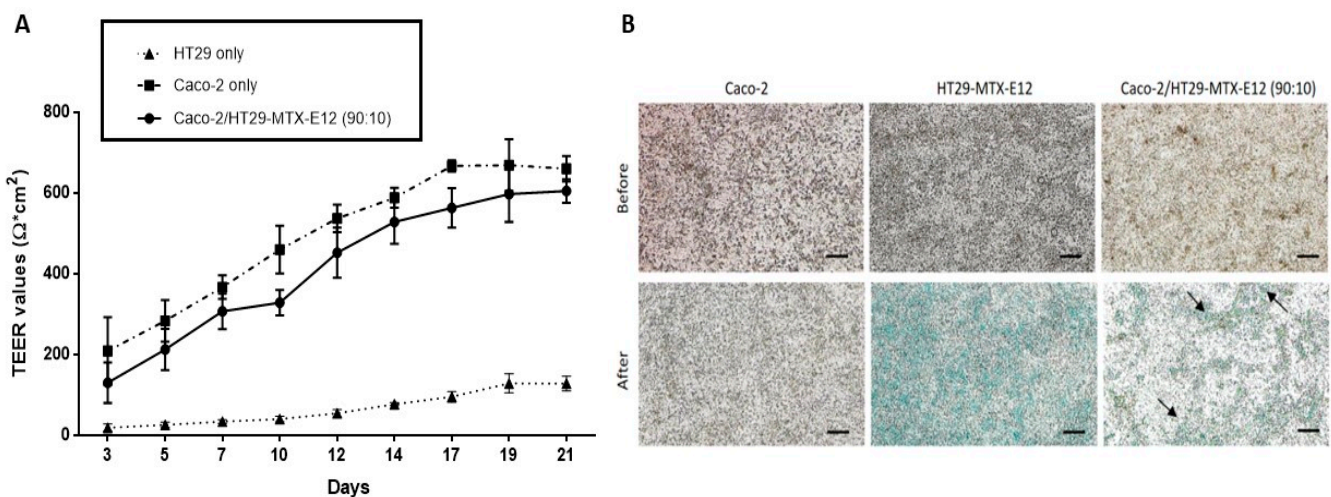


**Figure 3.** Characterization of the Caco-2/HT29-MTX-E12 (90:10 ratio) co-culture during 21 days of cultivation. (A) Transepithelial-transendothelial electrical resistance (TEER) values of Caco-2, HT29-MTX-E12, and Caco-2/HT29-MTX-E12 (90:10) cell cultures. Values are shown as mean  $\pm$  standard deviation (SD) ( $n \geq 3$ ). (B) Representative microscopy images of cell layers were obtained before and after staining with Alcian blue for mucus production (evident by blue color and black arrows). Scale bar = 100  $\mu$ m.

To determine the presence of mucus on the cell surface, the cell layers of 21-day cultured Caco-2, HT29-MTX-E12, and Caco-2/HT29-MTX-E12 (90:10 ratio) were stained with Alcian blue. Figure 3B shows that the Caco-2 monoculture did not exhibit Alcian blue staining. In contrast, as expected, the surface of HT29-MTX-E12 cells was covered by mucus production, while it was randomly dispersed throughout the cell layer of the Caco-2/HT29-MTX-E12 co-culture.

#### 2.4. Increased Intestinal Permeability in Caco-2/HT29-MTX-E12 Co-Culture Induced by IFN- $\gamma$ Priming

A previous study has reported that IFN- $\gamma$  priming resulted in the expression of TNF receptor 2, which was crucial for the subsequent induction of TNF- $\alpha$ -induced intestinal epithelial barrier dysfunction, caused by LPS [50]. Therefore, the Caco-2/HT29-MTX-E12 co-culture was primed here with IFN- $\gamma$  for 24 h, before the addition of the LPS-stimulated macrophage-like THP-1 cells, or primary monocyte-derived macrophages. As shown in Figure 4, IFN- $\gamma$  priming resulted in a significant drop in the TEER value (Figure 4A) and an increase in permeability (Figure 4B) as signs of barrier integrity loss. Compared to the untreated co-culture (SC), there was a TEER reduction of 25% and a permeability increase of around 18%.

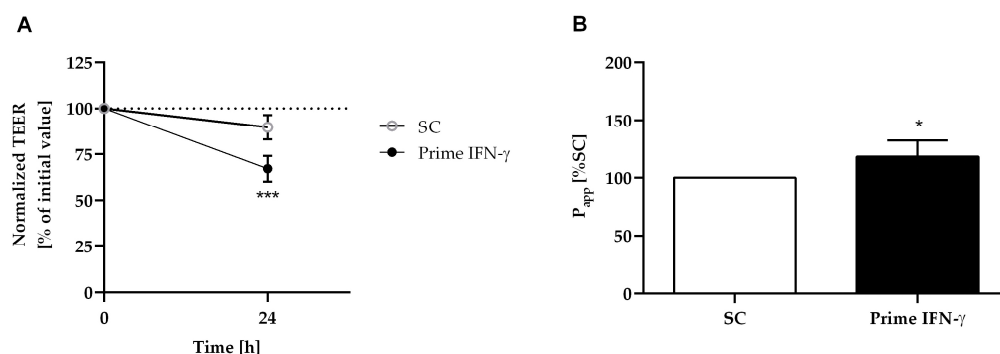


**Figure 4.** IFN- $\gamma$  priming on the Caco-2/HT29-MTX-E12 co-culture. After 24 h incubation with 50 ng/mL IFN- $\gamma$ , TEER (A) and permeability value ( $P_{app}$ ) (B) of Caco-2/HT29-MTX-E12 co-cultures were measured. TEER values were expressed as a percentage of the initial TEER value (100%). Permeability was expressed as fold change of the untreated control (SC) used as a reference. Bars are the means  $\pm$  SD ( $n \geq 3$ ). \*  $p < 0.05$ , or \*\*\*  $p < 0.001$  were considered significantly different versus SC.

#### 2.5. Characterization of the Inflammation-Triggered, Triple-Culture “Leaky Gut” Model

After 6 h and 24 h co-incubation with stimulated macrophage-like THP-1 cells, the intestinal barrier function of the Caco-2/HT29-MTX-E12 epithelial cell layer was assessed by measuring TEER (Figure 5A) and FITC-Dextran 4 kDa (FD4) paracellular transmission (Figure 5B). As seen in Figure 5A, within 6 h, the TEER of the “leaky gut” model decreased to 85% from the initial value, and further to 77% after 24 h. The paracellular flux of FD4 across the cellular layer showed a significantly increased permeability under “leaky gut” conditions, which was up to 41% and further to 71% higher than the control model after 6 h and 24 h, respectively (Figure 5B).

In comparison to the control model, significant release of the cytokines IL-6 and TNF- $\alpha$ , (insignificant for IL-1 $\beta$ ), was observed in the “leaky gut” model after 6 h (Figure 5C), and 24 h (Figure 5D). As seen in Figure 5C, after 6 h, the mean concentration of IL-6 and TNF- $\alpha$  in the “leaky gut” model were  $66 \pm 8$  pg/mL and  $163 \pm 72$  pg/mL, respectively. Those were significantly higher than levels of IL-6 and TNF- $\alpha$  in the control model ( $6 \pm 8$  pg/mL and  $41 \pm 22$  pg/mL, respectively). However, there was no significant difference in IL-1 $\beta$  production between the “leaky gut” and control models ( $16 \pm 8$  pg/mL and  $57 \pm 50$  pg/mL, respectively). Figure 5D also shows the significantly higher levels of IL-6 and TNF- $\alpha$  in the “leaky gut” model ( $77 \pm 26$  pg/mL and  $91 \pm 41$  pg/mL, respectively), as compared to the control model ( $11 \pm 4$  pg/mL and  $30 \pm 17$  pg/mL, respectively) after 24 h cultivation. Again, there was no significant difference in IL-1 $\beta$  production between the “leaky gut” and control models after 24 h ( $7 \pm 5$  pg/mL and  $20 \pm 13$  pg/mL, respectively).

The significant increased permeability highly corresponded to a significant production of zonulin, a proposed regulator of the permeability of the intestinal barrier [51], in the “leaky gut” model after 6 h (Figure 5E) and 24 h (Figure 5F). As seen in Figure 5E, within 6 h, the mean concentration of zonulin in both compartments of the “leaky gut” model ( $2043 \pm 464$  pg/mL)

was nearly 25-fold higher than in the control model ( $83 \pm 143$  pg/mL). After 24 h, the mean concentration of zonulin in both compartments of the “leaky gut” model ( $1982 \pm 260$  pg/mL) was around 1.3-fold higher than the control model ( $1664 \pm 29$  pg/mL) (Figure 5F).

As shown in Figure 5E,F, while there was no change in Tight Junction Protein-1 (TJP1) between the “leaky gut” and control models after 6 h ( $24 \pm 7$  pg/mL and  $22 \pm 8$  pg/mL, respectively) and 24 h ( $141 \pm 12$  pg/mL and  $147 \pm 6$  pg/mL, respectively), the amount of released occludin in the “leaky gut” model increased from  $66 \pm 13$  pg/mL at 6 h to  $104 \pm 49$  pg/mL at 24 h. On the other hand, the amount of occludin in the control model decreased from  $54 \pm 15$  pg/mL (6 h) to  $51 \pm 60$  pg/mL (24 h).

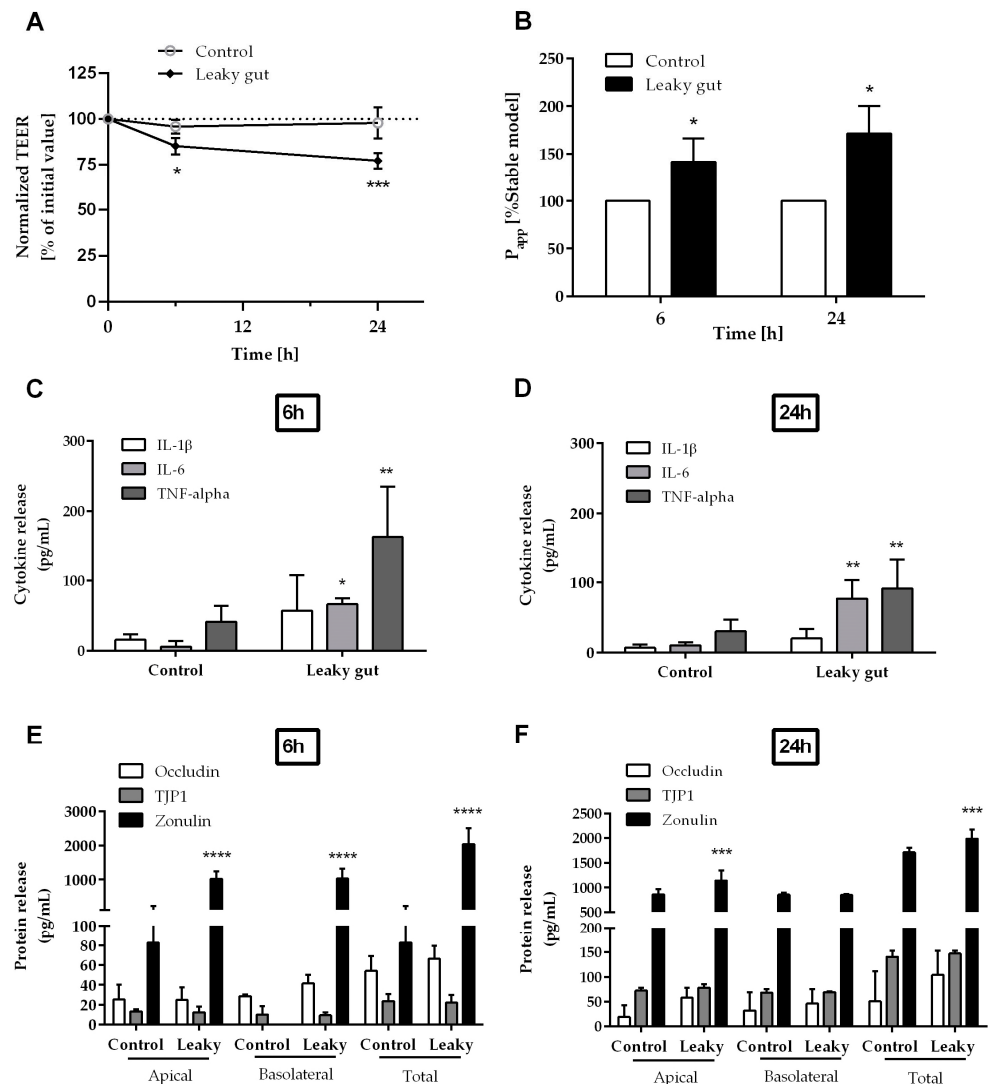


**Figure 5.** Characterization of the in vitro “leaky gut” model. Intestinal barrier function of the triple cell culture was assessed by (A) TEER and (B) permeability value ( $P_{app}$ ) after 6 h and 24 h incubation. The secretion of the key pro-inflammatory cytokines IL-1 $\beta$ , IL-6, and TNF- $\alpha$  in the basolateral compartment were quantified after (C) 6 h and (D) 24 h. The release of Occludin, Tight Junction Protein-1 (TJP1), and Zonulin in the apical, and basolateral compartment were measured after (E) 6 h and (F) 24 h. Data are given as mean  $\pm$  SD ( $n \geq 3$ ). \*  $p < 0.05$ , \*\*  $p < 0.01$ , \*\*\*  $p < 0.001$ , \*\*\*\*  $p < 0.0001$  as compared to the control model.

## 2.6. Comparison of Different Modifications on the “Leaky Gut” Model Using Macrophage-like THP-1 Cells

A previous study has described that increased intestinal permeability is correlated with increased levels of LPS in intestinal tissue and plasma [52]. Therefore, the “leaky gut” model was additionally treated with 100 ng/mL LPS in the apical compartment for 24 h. As shown in Figure 6, this modification resulted in a significant TEER drop of 30% (Figure 6A) and a permeability increase of 28% (Figure 6B) compared to the control model.

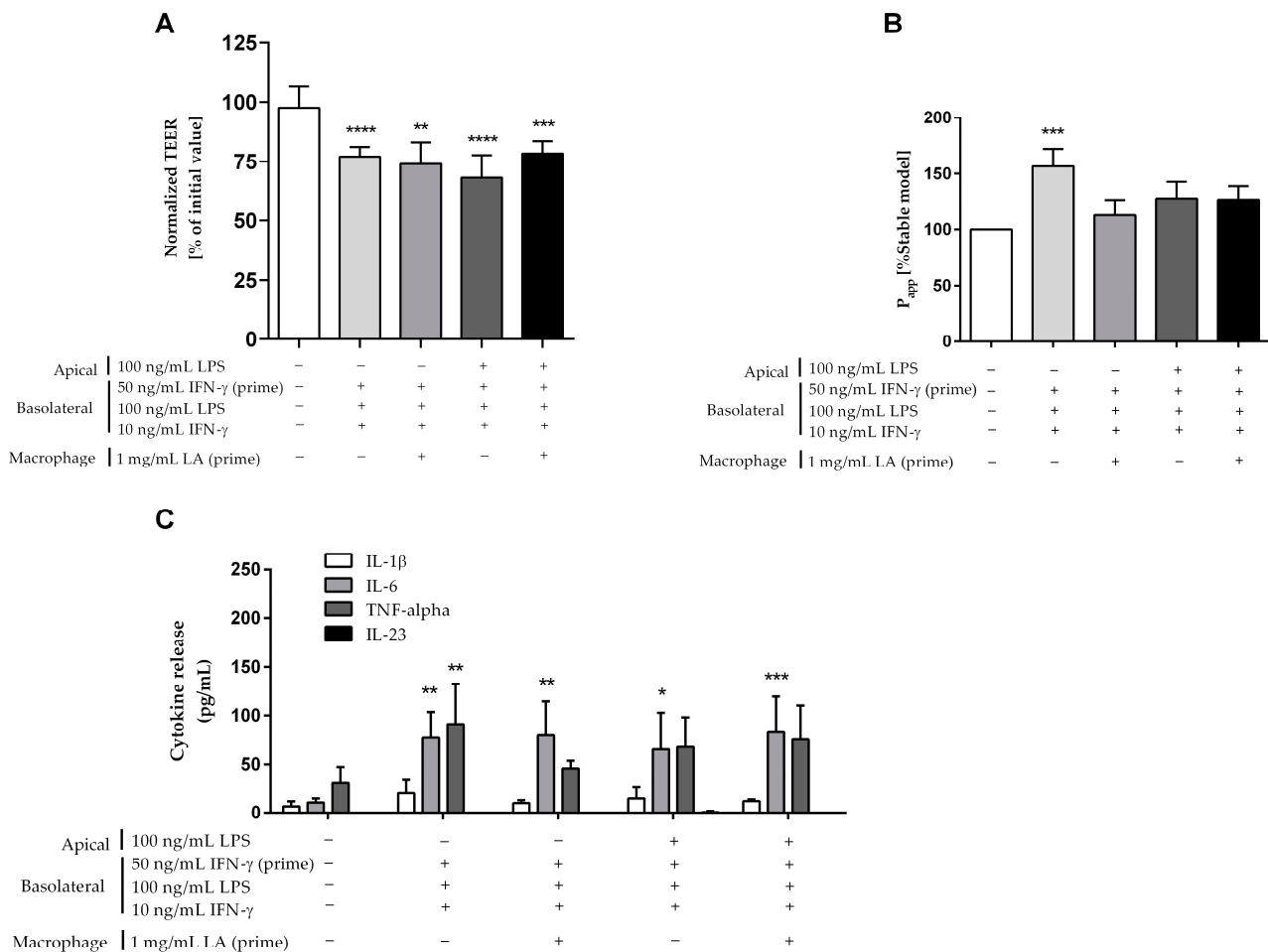


**Figure 6.** Comparison of different modifications on the “leaky gut” model using macrophage-like THP-1 cells (“-”: non-treatment, “+”: treatment). Intestinal barrier function was assessed by (A) TEER and (B) permeability value ( $P_{app}$ ) as compared to the control model. (C) The secretion of key pro-inflammatory cytokines IL-1 $\beta$ , IL-6, IL-23, and TNF- $\alpha$  was quantified in the basolateral compartment of the models after 24 h cultivation. Bars are mean  $\pm$  SD ( $n \geq 3$ ). \*  $p < 0.05$ , \*\*  $p < 0.01$ , \*\*\*  $p < 0.001$ , \*\*\*\*  $p < 0.0001$  as compared to the control model.

The cytokine interleukin-23 (IL-23), which is primarily produced by macrophages and dendritic cells in response to microbial stimulation, has been considered a key promoter of chronic intestinal inflammation, especially in IBD [53]. However, we could not detect IL-23 secretion in our model (Figure 6C). Lactic acid (LA) was reported as a stimulator of IL-23 production in PBMCs exposed to bacterial LPS [54]. Therefore, we pre-treated macrophage-like THP-1 cells with 1 mg/mL LA for 24 h before setting up the triple-culture. This modification showed a significant TEER reduction of approximately 24% (Figure 6A) and a permeability rise of 13% (Figure 6B) compared to the control model. The combination of the two modifications (apical treatment with LPS and LA priming) also resulted in a

significant TEER decrease of 20%, and a permeability increase of 27% as compared to the control model.

As described in Figure 6C, similar to the inflamed model, a significant secretion of IL-6 was found after additional modifications by using apical treatment of 100 ng/mL LPS ( $66 \pm 37$  pg/mL), or 24 h-priming of macrophage-like THP-1 cells with 1 mg/mL LA ( $79 \pm 35$  pg/mL), or the combination of these ( $83 \pm 37$  pg/mL) as compared to the control model ( $11 \pm 4$  pg/mL). There were similar levels in the production of IL-1 $\beta$ , TNF- $\alpha$ , and especially IL-23 between the modified “leaky gut” and control models.

### 2.7. Comparison of Different Modifications on the “Leaky Gut” Model Using Primary Human-Derived Macrophages

To better reflect the properties of primary macrophages in vivo, we replaced the THP-1 cell line in our model with primary monocyte-derived macrophages from human PBMCs. The experiments were then carried out as with the macrophage-like THP-1 cells.

The additional treatment with 100 ng/mL LPS in the apical compartment of the “leaky gut” model resulted in a significant TEER drop of 24% (Figure 7A) and a permeability increase of approximately 30% (Figure 7B) as compared to the control model.

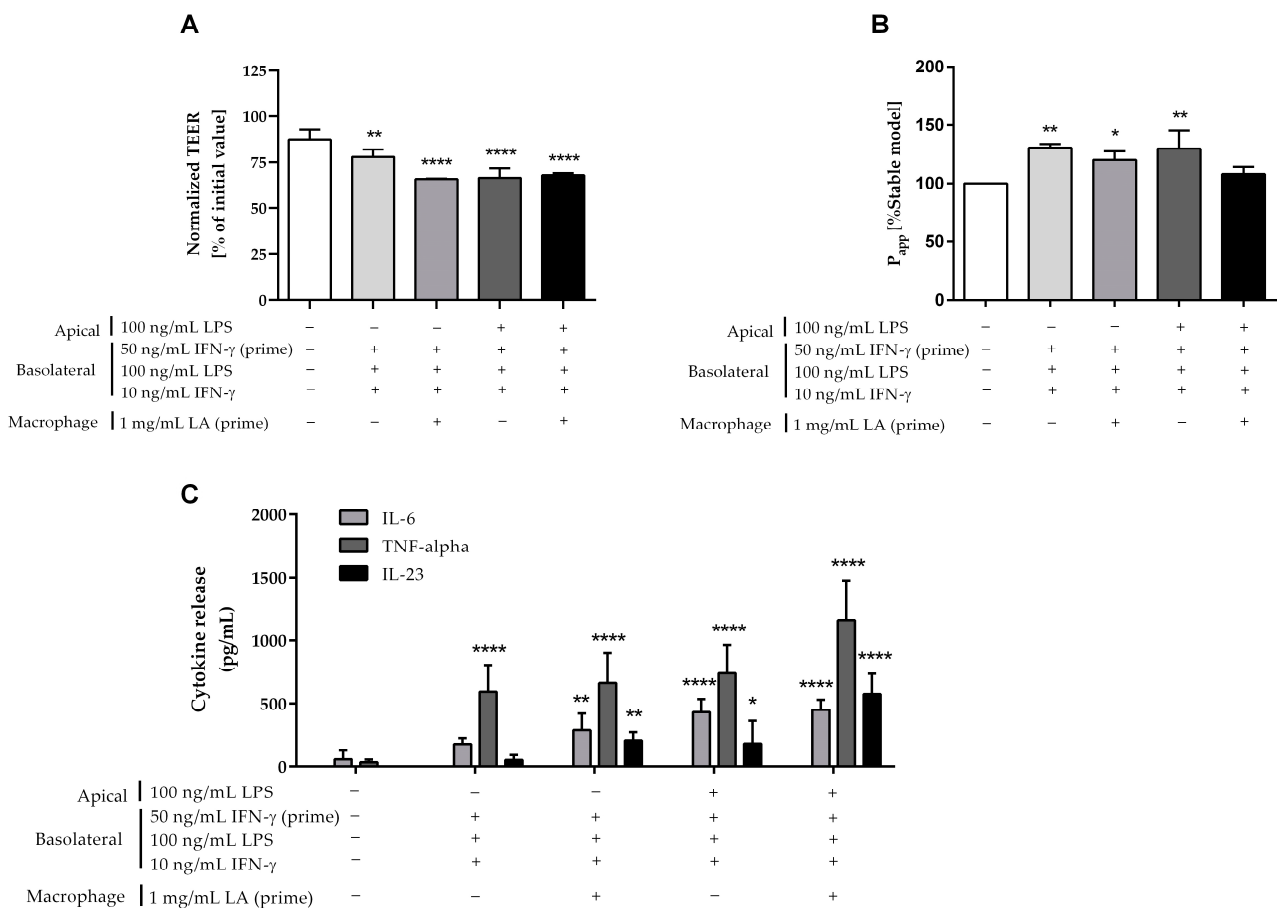


**Figure 7.** Comparison of the modifications on the “leaky gut” model using primary human-derived macrophages (“-”: non-treatment, “+”: treatment). Intestinal barrier function in comparison to the control model was assessed after 24 h by (A) TEER and (B) permeability values. (C) The secretion of key pro-inflammatory cytokines IL-6, IL-23, and TNF- $\alpha$  in the basolateral compartment of control and “leaky gut” models were quantified after 24 h. Bars are mean  $\pm$  SD ( $n \geq 3$ ). \*  $p < 0.05$ , \*\*  $p < 0.01$ , \*\*\*\*  $p < 0.0001$  as compared to the control model.

Similarly, 1 mg/mL LA pre-treatment of primary monocyte-derived macrophages for 24 h also caused a significant TEER reduction of 25% (Figure 7A), and a permeability rise of



20% (Figure 7B) in comparison with the control model. The combination of the two above modifications (apical treatment with LPS and LA priming) also resulted in a significant TEER decrease of 22%, but the permeability only slightly increased by 8% as compared to the control model.

As shown in Figure 7C, additional modifications with the apical treatment of 100 ng/mL LPS ( $433 \pm 102$  pg/mL), or 24 h-priming of macrophages with 1 mg/mL LA ( $290 \pm 130$  pg/mL), or the combination of these two modifications ( $451 \pm 80$  pg/mL) all produced a significant secretion of IL-6 in comparison with the control model ( $58 \pm 70$  pg/mL). Similarly, the substantial secretion in TNF- $\alpha$  was also seen by the apical treatment of 100 ng/mL LPS ( $741 \pm 223$  pg/mL), 24 h-priming macrophage with 1 mg/mL LA ( $662 \pm 240$  pg/mL), and the combination of these two modifications ( $1163 \pm 314$  pg/mL) as compared to the control model ( $34 \pm 21$  pg/mL). In contrast to macrophage-like THP-1 cells, the apical treatment with 100 ng/mL LPS ( $184 \pm 180$  pg/mL), or 24 h-priming of macrophages with 1 mg/mL LA ( $209 \pm 65$  pg/mL), or the combination of these two modifications ( $577 \pm 161$  pg/mL) resulted in a strong, significant secretion of IL-23 when compared to the control model (0 pg/mL).

### 3. Discussion

IBD is a chronic gastrointestinal inflammatory disease with unclear causes and pathogenesis. However, it is thought that a complex sequence of interactions among genetic, microbial, immunological, and environmental factors results in an abnormal and exaggerated immune response of the commensal microbiota, finally resulting in the induction of intestinal inflammation [55–58].

Various *in vitro* models have been developed to understand IBD's etiology, pathology, and potential treatment options. Most of them used the Caco-2 cell line, because differentiated Caco-2 cells can reflect many features of mature enterocytes in the intestinal epithelium, such as a brush border with microvilli, tight junction formation, production of characteristic digestive enzymes, and transporters [27]. Importantly, Caco-2 cells showed the ability to produce a range of inflammatory cytokines such as IL-6, IL-8, IL-1 $\beta$ , and TNF- $\alpha$ , that may contribute to inflammatory conditions in IBD [59]. Different studies have also utilized this cell line to evaluate novel molecules for potential therapeutic treatment/management of UC. For example, it was demonstrated, that rhamnolacturonan accelerated wound healing, decreased epithelial barrier dysfunction, and suppressed IL-1 induced IL-8 production in Caco-2 cells [60]. Another study by Liang et al. reported that the corn protein hydrolysate down-regulated the secretion of IL-8 production in TNF- $\alpha$  induced inflammation in Caco-2 cells [61].

Nevertheless, the most significant limitation of the monolayer Caco-2 cell culture system was the lack of a mucus layer, which serves as a physical and chemical barrier in the intestinal epithelium against luminal contents involving digestive enzymes, food particles, microbiota and microbial compounds, as well as host-secreted products such as bile acids [62]. Hence, previous studies co-cultured Caco-2 cells with the mucus-secreting goblet HT29-MTX-E12 cell line to provide a closer physiological model of the human intestinal epithelium [63–65]. Many recent studies have widely used the optimal 90:10 ratio of Caco-2/HT29-MTX cells, because it better represented the *in vivo* situation of the human small intestine regarding the proportion of absorptive enterocytes and mucin-producing goblet cells [66–69]. Therefore, we applied this combination of Caco-2/HT29-MTX-E12 co-culture conditions for our “leaky gut” model system to closely mimic the cell composition and functionality of the intestinal epithelium. In our model, the mucin secreted by the HT29-MTX cells does not appear to completely cover the whole surface of the intestinal cells after 21 days of co-culture. A healthy mucosal barrier contributes to the prevention of pathogens invasion and defects therein have been implicated in several intestinal pathologies. Thus, depending on the application of our *in vitro* model, this might be considered as a limitation or advantage.

Macrophages in the lamina propria of the small intestine are one of the most prevalent populations of leukocytes in the body. They play a crucial role in maintaining intestinal homeostasis and intestinal inflammation emergence [70]. Several investigations have demonstrated that intestinal macrophages become activated and promote the occurrence and development of IBD [35,37,71]. Over the last decade, to better replicate the *in vivo* physiology of IBD, *in vitro* IBD models have been established using a combination of Caco-2 cells and macrophage-like differentiated THP-1 cells, for example, Kämpfer et al. (2017) [46]. IFN- $\gamma$  priming of Caco-2 cells together with the stimulation of differentiated THP-1 cells by LPS and IFN- $\gamma$ , induced an inflammation-like response in their diseased intestine model, evident by intestinal barrier disruption and pro-inflammatory cytokine release. Based on this model of Kämpfer, co-culture models with differentiated Caco-2 cells and PMA-differentiated THP-1 cells in the presence of inflammatory stimulators (e.g., LPS with/without IFN- $\gamma$ ) have been used to evaluate the potential immunomodulatory and anti-inflammatory effects of phytochemicals [43,72,73], marine natural products [74–76], bacterial  $\beta$ -glucans [77], siRNA-based nanomedicine [42], bovine milk-derived extracellular vesicles [78], and probiotic bacteria [41].

Some IBD studies used an advanced *in vitro* triple-culture model composed of Caco-2 cells, HT29-MTX-(E12) cells, and PMA-differentiated macrophage-like THP-1 cells. The combination of two intestine cell lines (Caco-2/HT29-MTX) with differentiated THP-1 cells was first introduced by Kaulmann et al. (2016) to study the anti-inflammatory and antioxidant effects of plums and cabbages [79]. Busch et al. (2021) suggested that this advanced *in vitro* triple-culture model was a promising approach for studying the toxicological effects of ingested micro- and nano-plastic particles [80]. An adverse and pro-inflammatory role of the NLRP3 inflammasome in IBD has been described by using this triple-culture model [81].

However, this model system cannot reflect the anatomical distribution of lamina propria macrophages in humans, which are close to the epithelial monolayer of intestinal cells [70]. Thus, Calatayud et al. co-cultured Caco-2, HT29-MTX, and differentiated THP-1 cells in close contact [38]. In contrast to our model, they used Type I collagen from a rat tail to support THP-1 adhering to the membrane. Even though the presence of coated collagen could increase cell attachment and viability [82], it may potentially impact TEER measurements indirectly because the phenotyping properties of THP-1 cells were modified by the surrounding extracellular matrix (i.e., collagen Type I). Teplicky et al. have demonstrated that cell doubling times (i.e., cell proliferation) and mean diameters (i.e., cell size) of THP-1 cells in collagen Type I were slightly increased when compared to cells cultured in normal medium [83]. Furthermore, the biological activity of collagen-coated immune cells and the detection of released pro-inflammatory cytokines might also be affected [84]. Another study by Busch et al. (2021) also used a triple-culture model with close contact between intestinal cells (Caco-2/HT29-MTX-E12) and differentiated macrophage-like THP-1 cells [48]. They seeded Caco-2/HT29-MTX-E12 cells on the bottom side of the insert, while differentiated macrophage-like THP-1 cells were cultured on the top side of the insert. Due to the experimental design of their model, it is only suitable for studies with buoyant particles, which float in cell culture media due to their density of less than 1 g/cm<sup>3</sup>.

A significant increase in zonulin production could be observed in our “leaky gut” model when compared to the control model. Intestinal epithelial cell tight junctions are a multi-protein complex that support the integrity of the physical intestinal barrier by regulating the paracellular movement between the internal environment and external antigens or bacterial products [85,86]. It has been demonstrated that impaired tight junction proteins present an early event of IBD [87,88]. In fact, elevated levels of zonulin have been detected in both serum [89–91] and fecal [92,93] samples of IBD patients and it is used as biomarker of intestinal permeability of the small intestine [94,95]. Therefore, on this point our approach of a “leaky gut” model provides *in vitro* to *in vivo* concordance.

Cytokines play a critical role in the immunopathogenesis of IBD, where they regulate various aspects of the inflammatory response [96–98]. In patients with IBD, pro-

and anti-inflammatory cytokines have been demonstrated to be produced in the inflamed mucosa by various immune cells such as macrophages, dendritic cells (DCs), neutrophils, natural killer (NK) cells, intestinal epithelial cells (IECs), innate lymphoid cells (ILCs), mucosal effector T cells (T helper 1 (T<sub>H</sub>1), T<sub>H</sub>2 and T<sub>H</sub>17), and regulatory T (T<sub>reg</sub>) cells [99]. In particular, the translocation of commensal bacteria and microbial products from the gut lumen into the bowel wall resulting from an impaired cell barrier function (“leaky gut”) leads to inflammatory macrophage (M1 phenotype) stimulation, and consequent production of high levels of pro-inflammatory cytokines such as IL-1, IL-6, IL18, TNF- $\alpha$ , IL-23, and IL-17. These cytokines directly or indirectly result in the injury or necrosis of the intestinal epithelial cells, which then promotes the pathogenesis of IBD [35]. Being critical mediators in the development of IBD, pro-inflammatory cytokines are considered effective therapeutic targets [100,101]. Anti-TNF- $\alpha$  therapy is the first biologic approved, and currently the most effective treatment for IBD, including infliximab, golimumab, adalimumab, and certolizumab pegol, which have been demonstrated good clinical efficacy [102]. However, approximately 20% of IBD patients are primary non-responders [103], and over 30% eventually lose response to anti-TNF drugs [104]. Blocking of lamina propria macrophages-produced IL-6 with monoclonal antibodies (e.g., tocilizumab, PF-0423691) is here considered as alternative treatment for IBD, but serious side effects have been reported for these anti-IL-6 drugs [32].

More recent data have demonstrated, that the pro-inflammatory IL-23 was a critical promoter of the pathogenesis of IBD, because it stimulates and influences the differentiation and proliferation of pathogenic T helper type 17 (T<sub>H</sub>17) cells. This in turn further induces inflammatory cytokines [53,105,106]. Therefore, targeting the IL-23 pathway is another important way for drug development of IBD [107]. Currently, only ustekinumab has been approved for the treatment of both CD and UC patients, but several IL-23p19 antagonists (e.g., risankizumab, brazikumab, mirikizumab) are in phase II or III development programs and give promising results. Our “leaky gut” model showed a significant increase in IL-6 and TNF- $\alpha$  upon activation. Interestingly, we could also achieve the substantial secretion of IL-23 by additional modifications using primary human-derived macrophages, but not by using macrophage-like THP-1 cells. Since the exact mechanism by which lactic acid stimulates macrophages to release IL-23 is not fully understood, one possible reason for this difference could be correlated to the genetic and phenotypic differences between macrophage-like THP-1 cells, and primary blood macrophages. Compared to primary blood macrophages belonging to a non-malignant and non-proliferating cell type, THP-1 cells are leukemia monocytic cells with genetic and functional differences. Furthermore, concerning LPS responses, THP-1 cells express much lower levels of monocyte differentiation antigen CD14 in comparison to primary monocytes [108]. The detection of IL-23 has not yet been described in any other intestinal inflamed model before, thus our “leaky gut” model provides a promising new in vitro platform for drug investigation of IBD treatment, especially IL-23 pathway inhibitors.

## 4. Materials and Methods

### 4.1. Chemicals

Fetal calf serum (FCS), GlutaMAX<sup>TM</sup> supplement, Roswell Park Memorial Institute (RPMI)-1640, Dulbecco’s Modified Eagle’s medium (DMEM) with low glucose, trypsin-EDTA (0.5%), trypsin (2.5%) solution, phosphate-buffered saline (PBS, without Ca<sup>2+</sup> and Mg<sup>2+</sup>), Non-Essential Amino Acid (NEAA), penicillin/streptomycin solution (10,000 U/mL and 10,000  $\mu$ g/mL), StemPro<sup>TM</sup> Accutase<sup>TM</sup>, and Hank’s Balanced Salt Solution (HBSS) were purchased from Gibco<sup>TM</sup>, Life Technologies GmbH (Darmstadt, Germany). Lipopolysaccharide (LPS, from Escherichia coli O111:B4), phorbol 12-myristate 13-acetate (PMA), fluorescein isothiocyanate (FITC)-Dextran, Alcian blue 8GX solution (1% in 3% acetic acid) were from Sigma Aldrich (Taufkirchen, Germany). IFN- $\gamma$  (human recombinant) was purchased from STEMCELL technologies GmbH (Köln, Germany). Macrophage colony-stimulating factor (M-CSF) was purchased from Peprotech (Hamburg, Germany).

Paraformaldehyde (PFA) solution of 4% in PBS was purchased from Santa Cruz Biotechnology (Heidelberg, Germany).

#### 4.2. Cell Culture

The human colon carcinoma Caco-2 (ACC169) and HT29-MTX-E12-E12 cell lines were obtained from the German Collection of Microorganisms and Cell Cultures (DSMZ, Braunschweig, Germany) and European Collection of Authenticated Cell Cultures (Porton Down, UK), respectively. The cells were cultured separately in flasks in DMEM supplemented with 10% (*v/v*) FCS, 1% (*v/v*) NEAA, 100 U/mL penicillin, and 100 µg/mL streptomycin at 37 °C in a humidified incubator with a 5% CO<sub>2</sub>/95% air atmosphere. The culture medium was changed every 2–3 days and cells were regularly split at 90% confluence.

The THP-1 cell line was cultured in a flask in RPMI-1640 supplemented with 10% (*v/v*) FCS, 1% GlutaMAX™, 100 U/mL penicillin, and 100 µg/mL streptomycin at 37 °C in a humidified incubator with a 5% CO<sub>2</sub>/95% air atmosphere. THP-1 cells were maintained at a concentration between 0.2 to 1 × 10<sup>6</sup> cells/mL.

#### 4.3. Isolation and Cultivation of Human PBMCs

Human PBMCs were isolated from buffy coats of healthy volunteers at the University Medical Center in Freiburg, Germany by centrifugation on a LymphoPrep™ gradient (density: 1.077 g/cm<sup>3</sup>, 20 min, 500× *g*). Isolated PBMCs were cultured in complete RPMI 1640 medium supplemented with 10% heat-inactivated FCS, 2 mM L-glutamine, 100 U/mL penicillin, and 100 µg/mL streptomycin at 37 °C in a humidified incubator with a 5% CO<sub>2</sub>/95% air atmosphere.

#### 4.4. Co-Culture of Caco-2 and HT29-MTX-E12-E12 on Inserts

Monocultures of Caco-2 and HT29-MTX-E12 cells were harvested with Trypsin-EDTA and seeded on the apical chamber side of 12-well ThinCert® inserts (0.4 µm PET pore membrane, Greiner Bio-One, Frickenhausen, Germany) in an optimal proportion of 90:10, respectively, to reach a final density of 1 × 10<sup>5</sup> cells/cm<sup>2</sup>/insert. Cells were co-cultured for 19–21 days in a humidified incubator with a 5% CO<sub>2</sub>/95% air atmosphere with medium (0.5 mL on the apical side and 1.5 mL on the basolateral side) changed every 2–3 days.

#### 4.5. Macrophage Differentiation from THP-1 Cell Line and Peripheral Blood Primary Monocytes

THP-1 monocytes were seeded at 2 × 10<sup>5</sup> cells/mL in a 75 cm<sup>2</sup> flask and differentiated into macrophages by 72 h treated with 20 ng/mL PMA in a 5% CO<sub>2</sub>/95% air atmosphere incubator at 37 °C. After differentiation, the PMA-containing medium was discarded and the macrophage-like differentiated THP-1 were rested in fresh medium for 24 h.

Primary monocytes were purified from isolated PBMCs by using the culture plastic adherence technique: 2 × 10<sup>6</sup> isolated PBMCs/mL in complete medium were seeded into a 75 cm<sup>2</sup> culture flask and then monocytes were allowed to adhere at 37 °C in a 5% CO<sub>2</sub>/95% air atmosphere incubator. After 24 h incubation, non-adherent cells were removed from the flask. For macrophage differentiation, the adherent cells (mainly monocytes) were fed with the complete medium containing 50 ng/mL recombinant human M-CSF for additional 6 days in a 5% CO<sub>2</sub>/95% air atmosphere at 37 °C. The medium was then replaced every 3 days with fresh complete medium, supplemented with 50 ng/mL M-CSF. After that, monocyte-derived macrophages were rested in fresh medium for 24 h.

#### 4.6. Fabrication of 3D-Printed Cap for Insert

The caps were fabricated with a FormLabs 3+ 3D printer and BioMed Clear Resin, a USP class VI material used for medical devices that complies with ISO 18562. To avoid possible cross-contamination of the used materials, the caps were fabricated in an ISO 13485-certified laboratory with a printer that was solely used for the respective material. After printing, the caps were washed (Form Wash) and cured (Form Cure) according to the manufacturer's instructions (all devices and materials were purchased from FormLabs

GmbH, Berlin, Germany). The .stl file of the cap can be downloaded as supplemental material from the journal's homepage.

#### 4.7. Experimental Setup of the Inflammation-Triggered "Leaky Gut" Model

The control and inflammation-triggered or "leaky gut" Caco-2/HT29-MTX-E12-E12/THP-1 triple-culture was established as illustrated in Figure 1. Firstly, 19-day-differentiated Caco-2/HT29-MTX-E12-E12 epithelial cells in the apical compartment were either rested in fresh medium (control model) or primed with 50 ng/mL IFN- $\gamma$  for the inflammation-triggered model in 24 h before the triple-culture. On the next day, the medium from the basolateral side of the insert was completely discarded. The medium from the apical part was replaced with fresh medium, and a specially 3D-printed constructed cap was carefully placed into the insert (see Figure 2) to avoid the leakage of the medium during the following immune cell adherence procedure. The insert was placed upside down in a Petri dish. Then THP-1-differentiated macrophages ( $2 \times 10^5$  cells), or primary monocyte-derived macrophages ( $4 \times 10^4$  cells), which were initially detached from the 75 cm<sup>2</sup> culture flask with 50 ng/mL accutase, were transferred on the bottom side of the inverted inserts, for 1.5 h at 37 °C in a 5% CO<sub>2</sub> incubator. After immune cell adherence, the inserts were put back into 12-well plates in regular orientation before the specially 3D-printed constructed caps were carefully removed from the inserts. After medium removal, fresh medium was added to the upper and lower compartments of the insert. Macrophages from the control triple-culture were rested in fresh medium, while macrophages from the inflammation-triggered triple-culture were activated by 100 ng/mL LPS in combination with 10 ng/mL IFN- $\gamma$  for 24 h at 37 °C in a humidified incubator with a 5% CO<sub>2</sub>/95% air atmosphere.

To further optimize the "leaky gut" model, the treatment procedures involved some additional modifications. Condition 1: macrophage-like THP-1 cells were primed with 1 mg/mL lactic acid (LA) in 24 h before triple culture. Condition 2: the apical compartment was simultaneously treated with 100 ng/mL LPS during macrophage activation in the basolateral compartment. Condition 3: combination of conditions 1 and 2.

#### 4.8. Transepithelial Electrical Resistance Measurement

The cell monolayer integrity of the Caco-2/HT29-MTX-E12 co-culture on an insert was investigated using transepithelial electrical resistance (TEER) measurement. This measurement was performed by using an EVOM epithelial volt-ohmmeter equipped with a 'chopstick' electrode (STX-2) (Millicell<sup>®</sup> ERS, Millipore, Bedford, MA, USA). Before measurement, cells were stabilized at room temperature, while the electrode was sterilized with 70% ethanol and preconditioned in growth media. The measurement was performed in triplicates, and immediately after medium replacement. The final TEER value (TEER<sub>final</sub>) was corrected by subtracting the blank resistance (R<sub>blank</sub>) of the semipermeable membrane only (an insert without cells) from the resistance across the sample (R<sub>sample</sub>) before multiplying it by the effective growth area (A) of the insert.

$$\text{TEER}_{\text{final}} [\Omega \times \text{cm}^2] = (\text{R}_{\text{sample}} - \text{R}_{\text{blank}}) [\Omega] \times A [\text{cm}^2]$$

Co-culture inserts with TEER values over 300  $\Omega \cdot \text{cm}^2$  were used for further experiments. TEER results were expressed as a percentage of the initial TEER value.

#### 4.9. Alcian Blue Staining

Alcian Blue stain was used to visualize acidic epithelial and connective tissue mucins that were produced by HT29-MTX-E12 cells in the co-culture model. Briefly, Caco-2/HT29-MTX-E12 co-culture (90:10 ratio) was cultured at a density of  $1 \times 10^5$  cells/cm<sup>2</sup>/insert on 12-well plates for 21 days. After 21-day incubation, culture media were removed and cells were washed twice with pre-warmed PBS before they were fixed with 4% paraformaldehyde (PFA) for 30 min at room temperature. Next, PFA was aspirated and cells were rinsed with PBS twice before they were stained with 1% alcian blue in 3% acetic acid. After 30 min

incubation at room temperature, extra alcian blue was removed by two-time washing with PBS. The stained mucus was visualized by an inverted microscope (Fluorescence microscope Biozero BZ 8100E, Keyence GmbH, Neu-Isenburg, Germany).

#### 4.10. Permeability Studies

Paracellular permeability of the intestinal epithelium layer was determined using FITC-Dextran with a molecular weight of 4 kDa (FD4). Briefly, 250  $\mu$ L FD4 solution (1 mg/mL in HBSS), and 800  $\mu$ L HBSS was added to the apical and basolateral compartment, respectively. After 2 h incubation at 37  $^{\circ}$ C, 150  $\mu$ L from the basolateral side were transferred to a black 96-well plate (Greiner Bio-One, Frickenhausen, Germany). HBSS and FD4 solution were used as a negative and positive control, respectively. Fluorescence intensity was measured at excitation and emission wavelengths of 490 and 520 nm, respectively, by using a plate reader (TECAN infinite M200, Tecan trading AG, Männedorf, Switzerland). Permeability coefficient ( $P_{app}$ ) was calculated by using the following equation:

$$P_{app} = \frac{dQ}{dt} \times \frac{1}{A \times C_0}$$

Defined as:

$P_{app}$  = apparent permeability coefficient [cm/s].

$dQ/dt$  = rate of appearance of FD4 on the basolateral side [ $\mu$ g/s].

$A$  = surface area of the monolayer [cm<sup>2</sup>].

$C_0$  = initial FD4 concentration in the apical side [ $\mu$ g/mL].

#### 4.11. Tight Junction Proteins and Their Regulator Quantification

Cells were stimulated as described above. Secreted tight junction proteins (Occludin, Tight Junction Protein 1) and their regulator (Zonulin) in the supernatant were quantified by using specific ELISA kits (AssayGenie, Dublin, Ireland) according to the manufacturer's instructions. Results were standardized by comparison with a standard curve.

#### 4.12. Cytokine Level Measurement

Cells were stimulated as described above. Secreted proinflammatory cytokines (IL-1 $\beta$ , IL-6, IL-23, and TNF- $\alpha$ ) in the supernatant of the lower compartment were evaluated by using specific ELISA kits (Thermo Scientific, Darmstadt, Germany) according to the manufacturer's instructions. Results were standardized by comparison with a standard curve.

#### 4.13. Statistical Analysis

Results are expressed as the means  $\pm$  standard deviation (SD) of at least three independent experiments. When comparing between two groups, Student's unpaired  $t$  test was used. For experiments involving more than three groups, results were analyzed either by two-way ANOVA or two-way ANOVA followed by Tukey's multiple comparison tests. Data were analyzed using the GraphPad Prism version 6.07 software (GraphPad Software Inc., San Diego, CA, USA). Results were considered statistically significant when  $p < 0.05$ .

## 5. Conclusions

In conclusion, we described the establishment of a complex "leaky gut" model using epithelial cells (i.e., Caco-2), and mucus-secreting cells (i.e., HT29-MTX-E12) in close contact with activated immune cells (i.e., differentiated macrophage-like THP-1 cells or primary monocyte-derived macrophage) to simulate pathophysiological mechanisms of intestinal inflammation. Modifications on the original "leaky gut" model using primary human-derived macrophages, with either the additionally apical LPS treatment, or the LA pre-treatment of macrophages, further increased at least one of the "leaky gut" characteristics in our model. In particular, the expression of IL-23 could present a further advantage of this in vitro model. Even though there is no single model that can mimic all complex aspects of

IBD, we could address some limitations of previously established models. Therefore, our in vitro “leaky gut” model can provide a promising pre-clinical tool for novel IBD-related drug development and serve as an alternative system to in vivo animal testing.

**Supplementary Materials:** The supporting information can be downloaded at: <https://www.mdpi.com/article/10.3390/ijms24087427/s1>.

**Author Contributions:** E.L. and N.P.K.L. conceived and designed the study and experiments. N.P.K.L. and M.J.A. designed and carried out the experiments. N.P.K.L. and E.L. prepared the graphs and analyzed the data. N.P.K.L., E.L. and M.J.A. wrote the paper. All authors have read and agreed to the published version of the manuscript.

**Funding:** N.P.K.L. was funded by the German Academic Exchange Service (DAAD) through a Research Grant—Doctoral Programmes in Germany. The article processing charge was funded by the Baden-Württemberg Ministry of Science, Research and Art and the University of Freiburg in the funding program Open Access Publishing.

**Institutional Review Board Statement:** The experiments using human blood samples were conducted in accordance with the Declaration of Helsinki, and approved by the Ethics Committee of the University of Freiburg (protocol code 597/14 and 22-1466-S1, 17 January 2023).

**Informed Consent Statement:** Written informed consent was obtained from all subjects involved in the study.

**Data Availability Statement:** Not applicable.

**Acknowledgments:** The authors are especially thankful to Marie Czogalla for her support in the experiment of Alcian blue staining.

**Conflicts of Interest:** The authors declare no conflict of interest.

## References

1. Fukui, H. Increased Intestinal Permeability and Decreased Barrier Function: Does It Really Influence the Risk of Inflammation? *Inflamm. Intest. Dis.* **2016**, *1*, 135–145. [[CrossRef](#)]
2. Leech, B.; McIntyre, E.; Steel, A.; Sibbritt, D. Risk factors associated with intestinal permeability in an adult population: A systematic review. *Int. J. Clin. Pract.* **2019**, *73*, e13385. [[CrossRef](#)]
3. Vanuytsel, T.; Tack, J.; Farre, R. The Role of Intestinal Permeability in Gastrointestinal Disorders and Current Methods of Evaluation. *Front. Nutr.* **2021**, *8*, 717925. [[CrossRef](#)] [[PubMed](#)]
4. Fasano, A. Leaky gut and autoimmune diseases. *Clin. Rev. Allergy Immunol.* **2012**, *42*, 71–78. [[CrossRef](#)] [[PubMed](#)]
5. Mu, Q.; Kirby, J.; Reilly, C.M.; Luo, X.M. Leaky Gut As a Danger Signal for Autoimmune Diseases. *Front. Immunol.* **2017**, *8*, 598. [[CrossRef](#)] [[PubMed](#)]
6. Akdis, C.A. Does the epithelial barrier hypothesis explain the increase in allergy, autoimmunity and other chronic conditions? *Nat. Rev. Immunol.* **2021**, *21*, 739–751. [[CrossRef](#)] [[PubMed](#)]
7. Perrier, C.; Corthesy, B. Gut permeability and food allergies. *Clin. Exp. Allergy* **2011**, *41*, 20–28. [[CrossRef](#)]
8. Farshchi, M.K.; Azad, F.J.; Salari, R.; Mirsadraee, M.; Anushiravani, M. A Viewpoint on the Leaky Gut Syndrome to Treat Allergic Asthma: A Novel Opinion. *J. Evid. Based Complement. Altern. Med.* **2017**, *22*, 378–380. [[CrossRef](#)]
9. Fiorentino, M.; Sapone, A.; Senger, S.; Camhi, S.S.; Kadzielski, S.M.; Buie, T.M.; Kelly, D.L.; Cascella, N.; Fasano, A. Blood-brain barrier and intestinal epithelial barrier alterations in autism spectrum disorders. *Mol. Autism.* **2016**, *7*, 49. [[CrossRef](#)]
10. Kohler, O.; Krogh, J.; Mors, O.; Benros, M.E. Inflammation in Depression and the Potential for Anti-Inflammatory Treatment. *Curr. Neuropharmacol.* **2016**, *14*, 732–742. [[CrossRef](#)]
11. Obrenovich, M.E.M. Leaky Gut, Leaky Brain? *Microorganisms* **2018**, *6*, 107. [[CrossRef](#)] [[PubMed](#)]
12. Kushak, R.I.; Buie, T.M.; Murray, K.F.; Newburg, D.S.; Chen, C.; Nestoridi, E.; Winter, H.S. Evaluation of Intestinal Function in Children With Autism and Gastrointestinal Symptoms. *J. Pediatr. Gastroenterol. Nutr.* **2016**, *62*, 687–691. [[CrossRef](#)] [[PubMed](#)]
13. Yitik Tonkaz, G.; Esin, I.S.; Turan, B.; Uslu, H.; Dursun, O.B. Determinants of Leaky Gut and Gut Microbiota Differences in Children with Autism Spectrum Disorder and Their Siblings. *J. Autism. Dev. Disord.* **2022**, *1–14*. [[CrossRef](#)] [[PubMed](#)]
14. Jaworska, K.; Konop, M.; Bielinska, K.; Hutsch, T.; Dziekiewicz, M.; Banaszkiwicz, A.; Ufnal, M. Inflammatory bowel disease is associated with increased gut-to-blood penetration of short-chain fatty acids: A new, non-invasive marker of a functional intestinal lesion. *Exp. Physiol.* **2019**, *104*, 1226–1236. [[CrossRef](#)] [[PubMed](#)]
15. Michielan, A.; D’Inca, R. Intestinal Permeability in Inflammatory Bowel Disease: Pathogenesis, Clinical Evaluation, and Therapy of Leaky Gut. *Mediators. Inflamm.* **2015**, *2015*, 628157. [[CrossRef](#)]

16. Vindigni, S.M.; Zisman, T.L.; Suskind, D.L.; Damman, C.J. The intestinal microbiome, barrier function, and immune system in inflammatory bowel disease: A tripartite pathophysiological circuit with implications for new therapeutic directions. *Therap. Adv. Gastroenterol.* **2016**, *9*, 606–625. [[CrossRef](#)]
17. Collaborators, G.B.D.I.B.D. The global, regional, and national burden of inflammatory bowel disease in 195 countries and territories, 1990–2017: A systematic analysis for the Global Burden of Disease Study 2017. *Lancet Gastroenterol. Hepatol.* **2020**, *5*, 17–30. [[CrossRef](#)]
18. Kaplan, G.G.; Ng, S.C. Understanding and Preventing the Global Increase of Inflammatory Bowel Disease. *Gastroenterology* **2017**, *152*, 313–321. [[CrossRef](#)]
19. Kaplan, G.G. The global burden of IBD: From 2015 to 2025. *Nat. Rev. Gastroenterol. Hepatol.* **2015**, *12*, 720–727. [[CrossRef](#)]
20. Angelis, I.D.; Turco, L. Caco-2 cells as a model for intestinal absorption. *Curr. Protoc. Toxicol.* **2011**, *47*, 20.6.1–20.6.15. [[CrossRef](#)]
21. Cheng, K.C.; Li, C.; Uss, A.S. Prediction of oral drug absorption in humans—from cultured cell lines and experimental animals. *Expert. Opin. Drug Metab. Toxicol.* **2008**, *4*, 581–590. [[CrossRef](#)] [[PubMed](#)]
22. Liu, X.; Zheng, S.; Qin, Y.; Ding, W.; Tu, Y.; Chen, X.; Wu, Y.; Yanhua, L.; Cai, X. Experimental Evaluation of the Transport Mechanisms of PolIFN-alpha in Caco-2 Cells. *Front. Pharmacol.* **2017**, *8*, 781. [[CrossRef](#)] [[PubMed](#)]
23. Narayani, S.S.; Saravanan, S.; Ravindran, J.; Ramasamy, M.S.; Chitra, J. In vitro anticancer activity of fucoidan extracted from *Sargassum cinereum* against Caco-2 cells. *Int. J. Biol. Macromol.* **2019**, *138*, 618–628. [[CrossRef](#)] [[PubMed](#)]
24. Sevin, E.; Dehouck, L.; Fabulas-da Costa, A.; Cecchelli, R.; Dehouck, M.P.; Lundquist, S.; Culot, M. Accelerated Caco-2 cell permeability model for drug discovery. *J. Pharmacol. Toxicol. Methods* **2013**, *68*, 334–339. [[CrossRef](#)]
25. Shah, P.; Jogani, V.; Bagchi, T.; Misra, A. Role of Caco-2 cell monolayers in prediction of intestinal drug absorption. *Biotechnol. Prog.* **2006**, *22*, 186–198. [[CrossRef](#)]
26. Wang, Y.; Chen, X. QSPR model for Caco-2 cell permeability prediction using a combination of HQPSO and dual-RBF neural network. *RSC Adv.* **2020**, *10*, 42938–42952. [[CrossRef](#)]
27. Smetanova, L.; Stetinova, V.; Svoboda, Z.; Kvetina, J. Caco-2 cells, biopharmaceutics classification system (BCS) and biowaiver. *Acta. Medica.* **2011**, *54*, 3–8.
28. Simon-Assmann, P.; Turck, N.; Sidhoum-Jenny, M.; Gradwohl, G.; Kedinger, M. In vitro models of intestinal epithelial cell differentiation. *Cell Biol. Toxicol.* **2007**, *23*, 241–256. [[CrossRef](#)]
29. Panse, N.; Gerk, P.M. The Caco-2 Model: Modifications and enhancements to improve efficiency and predictive performance. *Int. J. Pharm.* **2022**, *624*, 122004. [[CrossRef](#)]
30. Martinez-Maqueda, D.; Miralles, B.; Recio, I. HT29 Cell Line. In *The Impact of Food Bioactives on Health: In Vitro and Ex Vivo Models*; Verhoeckx, K., Cotter, P., Kleiveland, C., Mackie, A., Swiatecka, D., Eds.; Springer: Cham, Switzerland, 2015; pp. 113–124. [[CrossRef](#)]
31. Corfield, A.P.; Carroll, D.; Myerscough, N.; Probert, C.S. Mucins in the gastrointestinal tract in health and disease. *Front. Biosci.* **2001**, *6*, D1321–D1357. [[CrossRef](#)]
32. Boegh, M.; Nielsen, H.M. Mucus as a barrier to drug delivery—Understanding and mimicking the barrier properties. *Basic Clin. Pharmacol. Toxicol.* **2015**, *116*, 179–186. [[CrossRef](#)] [[PubMed](#)]
33. Fang, J.; Wang, H.; Zhou, Y.; Zhang, H.; Zhou, H.; Zhang, X. Slimy partners: The mucus barrier and gut microbiome in ulcerative colitis. *Exp. Mol. Med.* **2021**, *53*, 772–787. [[CrossRef](#)] [[PubMed](#)]
34. Fernandez-Tome, S.; Ortega Moreno, L.; Chaparro, M.; Gisbert, J.P. Gut Microbiota and Dietary Factors as Modulators of the Mucus Layer in Inflammatory Bowel Disease. *Int. J. Mol. Sci.* **2021**, *22*, 10224. [[CrossRef](#)] [[PubMed](#)]
35. Han, X.; Ding, S.; Jiang, H.; Liu, G. Roles of Macrophages in the Development and Treatment of Gut Inflammation. *Front. Cell Dev. Biol.* **2021**, *9*, 625423. [[CrossRef](#)]
36. Hine, A.M.; Loke, P. Intestinal Macrophages in Resolving Inflammation. *J. Immunol.* **2019**, *203*, 593–599. [[CrossRef](#)]
37. Na, Y.R.; Stakenborg, M.; Seok, S.H.; Matteoli, G. Macrophages in intestinal inflammation and resolution: A potential therapeutic target in IBD. *Nat. Rev. Gastroenterol. Hepatol.* **2019**, *16*, 531–543. [[CrossRef](#)] [[PubMed](#)]
38. Calatayud, M.; Dezutter, O.; Hernandez-Sanabria, E.; Hidalgo-Martinez, S.; Meysman, F.J.R.; Van de Wiele, T. Development of a host-microbiome model of the small intestine. *FASEB J.* **2019**, *33*, 3985–3996. [[CrossRef](#)] [[PubMed](#)]
39. Kämpfer, A.A.; Shah, U.K.; Chu, S.L.; Busch, M.; Büttner, V.; He, R.; Rothen-Rutishauser, B.; Schins, R.P.; Jenkins, G.J. Inter-laboratory comparison of an intestinal triple culture to confirm transferability and reproducibility. *In Vitro Model.* **2022**, *1*–9. [[CrossRef](#)]
40. Ponce de Leon-Rodriguez, M.D.C.; Guyot, J.P.; Laurent-Babot, C. Intestinal in vitro cell culture models and their potential to study the effect of food components on intestinal inflammation. *Crit. Rev. Food Sci. Nutr.* **2019**, *59*, 3648–3666. [[CrossRef](#)]
41. Foey, A.; Habil, N.; Strachan, A.; Beal, J. Lacticaseibacillus casei Strain Shirota Modulates Macrophage-Intestinal Epithelial Cell Co-Culture Barrier Integrity, Bacterial Sensing and Inflammatory Cytokines. *Microorganisms* **2022**, *10*, 2087. [[CrossRef](#)]
42. Hartwig, O.; Loretz, B.; Nougarede, A.; Jary, D.; Sulpice, E.; Gidrol, X.; Navarro, F.; Lehr, C.M. Leaky gut model of the human intestinal mucosa for testing siRNA-based nanomedicine targeting JAK1. *J. Control Release* **2022**, *345*, 646–660. [[CrossRef](#)] [[PubMed](#)]
43. Kordulewska, N.K.; Topa, J.; Tanska, M.; Cieslinska, A.; Fiedorowicz, E.; Savelkoul, H.F.J.; Jarmolowska, B. Modulatory Effects of Osthole on Lipopolysaccharides-Induced Inflammation in Caco-2 Cell Monolayer and Co-Cultures with THP-1 and THP-1-Derived Macrophages. *Nutrients* **2020**, *13*, 123. [[CrossRef](#)] [[PubMed](#)]



44. Schnur, S.; Wahl, V.; Metz, J.K. Inflammatory bowel disease addressed by Caco-2 and monocyte-derived macrophages: An opportunity for an in vitro drug screening assay. *In Vitro Model.* **2022**, *1*, 363–383. [[CrossRef](#)]
45. Kampf, A.A.M.; Busch, M.; Buttner, V.; Bredeck, G.; Stahlmecke, B.; Hellack, B.; Masson, I.; Sofranko, A.; Albrecht, C.; Schins, R.P.F. Model Complexity as Determining Factor for In Vitro Nanosafety Studies: Effects of Silver and Titanium Dioxide Nanomaterials in Intestinal Models. *Small* **2021**, *17*, e2004223. [[CrossRef](#)] [[PubMed](#)]
46. Kampf, A.A.M.; Urban, P.; Gioria, S.; Kanase, N.; Stone, V.; Kinsner-Ovaskainen, A. Development of an in vitro co-culture model to mimic the human intestine in healthy and diseased state. *Toxicol. In Vitro* **2017**, *45*, 31–43. [[CrossRef](#)]
47. Maescotti, D.; Lo Sasso, G.; Guerrera, D.; Renggli, K.; Ruiz Castro, P.A.; Piault, R.; Jaquet, V.; Moine, F.; Luettich, K.; Frenzel, S.; et al. Development of an Advanced Multicellular Intestinal Model for Assessing Immunomodulatory Properties of Anti-Inflammatory Compounds. *Front. Pharmacol.* **2021**, *12*, 639716. [[CrossRef](#)]
48. Busch, M.; Kampf, A.A.M.; Schins, R.P.F. An inverted in vitro triple culture model of the healthy and inflamed intestine: Adverse effects of polyethylene particles. *Chemosphere* **2021**, *284*, 131345. [[CrossRef](#)]
49. Srinivasan, B.; Kolli, A.R.; Esch, M.B.; Abaci, H.E.; Shuler, M.L.; Hickman, J.J. TEER measurement techniques for in vitro barrier model systems. *J. Lab. Autom.* **2015**, *20*, 107–126. [[CrossRef](#)]
50. Wang, F.; Graham, W.V.; Wang, Y.; Witkowski, E.D.; Schwarz, B.T.; Turner, J.R. Interferon-gamma and tumor necrosis factor-alpha synergize to induce intestinal epithelial barrier dysfunction by up-regulating myosin light chain kinase expression. *Am. J. Pathol.* **2005**, *166*, 409–419. [[CrossRef](#)]
51. Fasano, A. Intestinal permeability and its regulation by zonulin: Diagnostic and therapeutic implications. *Clin. Gastroenterol. Hepatol.* **2012**, *10*, 1096–1100. [[CrossRef](#)]
52. Andreassen, A.S.; Krabbe, K.S.; Krogh-Madsen, R.; Taudorf, S.; Pedersen, B.K.; Moller, K. Human endotoxemia as a model of systemic inflammation. *Curr. Med. Chem.* **2008**, *15*, 1697–1705. [[CrossRef](#)] [[PubMed](#)]
53. Sewell, G.W.; Kaser, A. Interleukin-23 in the Pathogenesis of Inflammatory Bowel Disease and Implications for Therapeutic Intervention. *J. Crohns. Colitis.* **2022**, *16*, ii3–ii19. [[CrossRef](#)] [[PubMed](#)]
54. Witkin, S.S.; Alvi, S.; Bongiovanni, A.M.; Linhares, I.M.; Ledger, W.J. Lactic acid stimulates interleukin-23 production by peripheral blood mononuclear cells exposed to bacterial lipopolysaccharide. *FEMS Immunol. Med. Microbiol.* **2011**, *61*, 153–158. [[CrossRef](#)] [[PubMed](#)]
55. Ananthakrishnan, A.N.; Bernstein, C.N.; Iliopoulos, D.; Macpherson, A.; Neurath, M.F.; Ali, R.A.R.; Vavricka, S.R.; Fiocchi, C. Environmental triggers in IBD: A review of progress and evidence. *Nat. Rev. Gastroenterol. Hepatol.* **2018**, *15*, 39–49. [[CrossRef](#)]
56. Khor, B.; Gardet, A.; Xavier, R.J. Genetics and pathogenesis of inflammatory bowel disease. *Nature* **2011**, *474*, 307–317. [[CrossRef](#)]
57. Liu, T.C.; Stappenbeck, T.S. Genetics and Pathogenesis of Inflammatory Bowel Disease. *Annu. Rev. Pathol.* **2016**, *11*, 127–148. [[CrossRef](#)]
58. Wallace, K.L.; Zheng, L.B.; Kanazawa, Y.; Shih, D.Q. Immunopathology of inflammatory bowel disease. *World J. Gastroenterol.* **2014**, *20*, 6–21. [[CrossRef](#)]
59. Andrews, C.; McLean, M.H.; Durum, S.K. Cytokine Tuning of Intestinal Epithelial Function. *Front. Immunol.* **2018**, *9*, 1270. [[CrossRef](#)]
60. Maria-Ferreira, D.; Nascimento, A.M.; Cipriani, T.R.; Santana-Filho, A.P.; Watanabe, P.D.S.; Sant Ana, D.M.G.; Luciano, F.B.; Bocate, K.C.P.; van den Wijngaard, R.M.; Werner, M.F.P.; et al. Rhamnogalacturonan, a chemically-defined polysaccharide, improves intestinal barrier function in DSS-induced colitis in mice and human Caco-2 cells. *Sci. Rep.* **2018**, *8*, 12261. [[CrossRef](#)]
61. Liang, Q.; Ren, X.; Chalamaiiah, M.; Ma, H. Simulated gastrointestinal digests of corn protein hydrolysate alleviate inflammation in caco-2 cells and a mouse model of colitis. *J. Food Sci. Technol.* **2020**, *57*, 2079–2088. [[CrossRef](#)]
62. Johansson, M.E.; Larsson, J.M.; Hansson, G.C. The two mucus layers of colon are organized by the MUC2 mucin, whereas the outer layer is a legislator of host-microbial interactions. *Proc. Natl. Acad. Sci. USA* **2011**, *108* (Suppl. S1), 4659–4665. [[CrossRef](#)] [[PubMed](#)]
63. Chen, X.M.; Elisia, I.; Kitts, D.D. Defining conditions for the co-culture of Caco-2 and HT29-MTX cells using Taguchi design. *J. Pharmacol. Toxicol. Methods* **2010**, *61*, 334–342. [[CrossRef](#)] [[PubMed](#)]
64. Lozoya-Agullo, I.; Araujo, F.; Gonzalez-Alvarez, I.; Merino-Sanjuan, M.; Gonzalez-Alvarez, M.; Bermejo, M.; Sarmiento, B. Usefulness of Caco-2/HT29-MTX and Caco-2/HT29-MTX/Raji B Coculture Models To Predict Intestinal and Colonic Permeability Compared to Caco-2 Monoculture. *Mol. Pharm.* **2017**, *14*, 1264–1270. [[CrossRef](#)] [[PubMed](#)]
65. Pan, F.; Han, L.; Zhang, Y.; Yu, Y.; Liu, J. Optimization of Caco-2 and HT29 co-culture in vitro cell models for permeability studies. *Int. J. Food Sci. Nutr.* **2015**, *66*, 680–685. [[CrossRef](#)]
66. Barnett, A.M.; Roy, N.C.; Cookson, A.L.; McNabb, W.C. Metabolism of Caprine Milk Carbohydrates by Probiotic Bacteria and Caco-2:HT29(-)MTX Epithelial Co-Cultures and Their Impact on Intestinal Barrier Integrity. *Nutrients* **2018**, *10*, 949. [[CrossRef](#)]
67. Garcia-Rodriguez, A.; Vila, L.; Cortes, C.; Hernandez, A.; Marcos, R. Effects of differently shaped TiO<sub>2</sub>NPs (nanospheres, nanorods and nanowires) on the in vitro model (Caco-2/HT29) of the intestinal barrier. *Part. Fibre. Toxicol.* **2018**, *15*, 33. [[CrossRef](#)]
68. Hu, W.; Feng, P.; Zhang, M.; Tian, T.; Wang, S.; Zhao, B.; Li, Y.; Wang, S.; Wu, C. Endotoxins Induced ECM-Receptor Interaction Pathway Signal Effect on the Function of MUC2 in Caco2/HT29 Co-Culture Cells. *Front. Immunol.* **2022**, *13*, 916933. [[CrossRef](#)]
69. Le, N.P.K.; Herz, C.; Gomes, J.V.D.; Forster, N.; Antoniadou, K.; Mittermeier-Klessinger, V.K.; Mewis, I.; Dawid, C.; Ulrichs, C.; Lamy, E. Comparative Anti-Inflammatory Effects of Salix Cortex Extracts and Acetylsalicylic Acid in SARS-CoV-2 Peptide and LPS-Activated Human In Vitro Systems. *Int. J. Mol. Sci.* **2021**, *22*, 6766. [[CrossRef](#)]

70. Bain, C.C.; Mowat, A.M. Macrophages in intestinal homeostasis and inflammation. *Immunol. Rev.* **2014**, *260*, 102–117. [[CrossRef](#)]
71. Geremia, A.; Arancibia-Carcamo, C.V. Innate Lymphoid Cells in Intestinal Inflammation. *Front. Immunol.* **2017**, *8*, 1296. [[CrossRef](#)]
72. Liu, L.; Lu, Y.; Xu, C.; Chen, H.; Wang, X.; Wang, Y.; Cai, B.; Li, B.; Verstrepen, L.; Ghyselinck, J.; et al. The Modulation of Chaihu Shugan Formula on Microbiota Composition in the Simulator of the Human Intestinal Microbial Ecosystem Technology Platform and its Influence on Gut Barrier and Intestinal Immunity in Caco-2/THP1-Blue Cell Co-Culture Model. *Front. Pharmacol.* **2022**, *13*, 820543. [[CrossRef](#)] [[PubMed](#)]
73. Stevens, Y.; de Bie, T.; Pinheiro, I.; Elizalde, M.; Masclee, A.; Jonkers, D. The effects of citrus flavonoids and their metabolites on immune-mediated intestinal barrier disruption using an in vitro co-culture model. *Br. J. Nutr.* **2022**, *128*, 1917–1926. [[CrossRef](#)] [[PubMed](#)]
74. Ji, Y.K.; Lee, S.M.; Kim, N.H.; Tu, N.V.; Kim, Y.N.; Heo, J.D.; Jeong, E.J.; Rho, J.R. Stereochemical Determination of Fistularins Isolated from the Marine Sponge *Ecionemia acervus* and Their Regulatory Effect on Intestinal Inflammation. *Mar. Drugs* **2021**, *19*, 170. [[CrossRef](#)] [[PubMed](#)]
75. Kim, Y.N.; Ji, Y.K.; Kim, N.H.; Van Tu, N.; Rho, J.R.; Jeong, E.J. Isoquinolinequinone Derivatives from a Marine Sponge (*Haliclona* sp.) Regulate Inflammation in In Vitro System of Intestine. *Mar. Drugs* **2021**, *19*, 90. [[CrossRef](#)] [[PubMed](#)]
76. Lee, S.M.; Kim, N.H.; Lee, S.; Kim, Y.N.; Heo, J.D.; Rho, J.R.; Jeong, E.J. (10Z)-Debromohymenialdisine from Marine Sponge *Stylissa* sp. Regulates Intestinal Inflammatory Responses in Co-Culture Model of Epithelial Caco-2 Cells and THP-1 Macrophage Cells. *Molecules* **2019**, *24*, 3394. [[CrossRef](#)]
77. Notararigo, S.; Varela, E.; Otal, A.; Antolin, M.; Guarner, F.; Lopez, P. Anti-Inflammatory Effect of an O-2-Substituted (1-3)-beta-D-Glucan Produced by *Pediococcus parvulus* 2.6 in a Caco-2 PMA-THP-1 Co-Culture Model. *Int. J. Mol. Sci.* **2022**, *23*, 1527. [[CrossRef](#)]
78. Mecocci, S.; Ottaviani, A.; Razzuoli, E.; Fiorani, P.; Pietrucci, D.; De Ciucis, C.G.; Dei Giudici, S.; Franzoni, G.; Chillemi, G.; Cappelli, K. Cow Milk Extracellular Vesicle Effects on an In Vitro Model of Intestinal Inflammation. *Biomedicines* **2022**, *10*, 570. [[CrossRef](#)]
79. Kaulmann, A.; Legay, S.; Schneider, Y.J.; Hoffmann, L.; Bohn, T. Inflammation related responses of intestinal cells to plum and cabbage digesta with differential carotenoid and polyphenol profiles following simulated gastrointestinal digestion. *Mol. Nutr. Food Res.* **2016**, *60*, 992–1005. [[CrossRef](#)]
80. Busch, M.; Bredeck, G.; Kampfer, A.A.M.; Schins, R.P.F. Investigations of acute effects of polystyrene and polyvinyl chloride micro- and nanoplastics in an advanced in vitro triple culture model of the healthy and inflamed intestine. *Environ. Res.* **2021**, *193*, 110536. [[CrossRef](#)]
81. Busch, M.; Ramachandran, H.; Wahle, T.; Rossi, A.; Schins, R.P.F. Investigating the Role of the NLRP3 Inflammasome Pathway in Acute Intestinal Inflammation: Use of THP-1 Knockout Cell Lines in an Advanced Triple Culture Model. *Front. Immunol.* **2022**, *13*, 898039. [[CrossRef](#)]
82. Park, B.U.; Park, S.M.; Lee, K.P.; Lee, S.J.; Nam, Y.E.; Park, H.S.; Eom, S.; Lim, J.O.; Kim, D.S.; Kim, H.K. Collagen immobilization on ultra-thin nanofiber membrane to promote in vitro endothelial monolayer formation. *J. Tissue Eng.* **2019**, *10*, 2041731419887833. [[CrossRef](#)] [[PubMed](#)]
83. Teplicky, T.; Mateasik, A.; Balazsiova, Z.; Kajo, K.; Vallova, M.; Filova, B.; Trnka, M.; Cunderlikova, B. Phenotypical modifications of immune cells are enhanced by extracellular matrix. *Exp. Cell. Res.* **2021**, *405*, 112710. [[CrossRef](#)] [[PubMed](#)]
84. Vaday, G.G.; Lider, O. Extracellular matrix moieties, cytokines, and enzymes: Dynamic effects on immune cell behavior and inflammation. *J. Leukoc. Biol.* **2000**, *67*, 149–159. [[CrossRef](#)]
85. Turner, J.R. Intestinal mucosal barrier function in health and disease. *Nat. Rev. Immunol.* **2009**, *9*, 799–809. [[CrossRef](#)] [[PubMed](#)]
86. Zihni, C.; Mills, C.; Matter, K.; Balda, M.S. Tight junctions: From simple barriers to multifunctional molecular gates. *Nat. Rev. Mol. Cell Biol.* **2016**, *17*, 564–580. [[CrossRef](#)]
87. Lechuga, S.; Ivanov, A.I. Disruption of the epithelial barrier during intestinal inflammation: Quest for new molecules and mechanisms. *Biochim. Biophys. Acta Mol. Cell Res.* **2017**, *1864*, 1183–1194. [[CrossRef](#)] [[PubMed](#)]
88. Lee, B.; Moon, K.M.; Kim, C.Y. Tight Junction in the Intestinal Epithelium: Its Association with Diseases and Regulation by Phytochemicals. *J. Immunol. Res.* **2018**, *2018*, 2645465. [[CrossRef](#)] [[PubMed](#)]
89. Caviglia, G.P.; Dughera, F.; Ribaldone, D.G.; Rosso, C.; Abate, M.L.; Pellicano, R.; Bresso, F.; Smedile, A.; Saracco, G.M.; Astegiano, M. Serum zonulin in patients with inflammatory bowel disease: A pilot study. *Minerva. Med.* **2019**, *110*, 95–100. [[CrossRef](#)]
90. Wang, X.; Memon, A.A.; Palmer, K.; Hedelius, A.; Sundquist, J.; Sundquist, K. The association of zonulin-related proteins with prevalent and incident inflammatory bowel disease. *BMC Gastroenterol.* **2022**, *22*, 3. [[CrossRef](#)]
91. Lacombe, L.A.C.; Matiollo, C.; Rosa, J.S.D.; Felisberto, M.; Dalmarco, E.M.; Schiavon, L.L. Factors Associated with Circulating Zonulin in Inflammatory Bowel Disease. *Arq. Gastroenterol.* **2022**, *59*, 238–243. [[CrossRef](#)]
92. Szymanska, E.; Wierzbicka, A.; Dadalski, M.; Kierkus, J. Fecal Zonulin as a Noninvasive Biomarker of Intestinal Permeability in Pediatric Patients with Inflammatory Bowel Diseases-Correlation with Disease Activity and Fecal Calprotectin. *J. Clin. Med.* **2021**, *10*, 3905. [[CrossRef](#)] [[PubMed](#)]
93. Malickova, K.; Francova, I.; Lukas, M.; Kolar, M.; Kralikova, E.; Bortlik, M.; Duricova, D.; Stepankova, L.; Zvolaska, K.; Pankova, A.; et al. Fecal zonulin is elevated in Crohn's disease and in cigarette smokers. *Pract. Lab. Med.* **2017**, *9*, 39–44. [[CrossRef](#)] [[PubMed](#)]

94. Fasano, A. Zonulin, regulation of tight junctions, and autoimmune diseases. *Ann. N. Y. Acad. Sci.* **2012**, *1258*, 25–33. [[CrossRef](#)]
95. Sturgeon, C.; Fasano, A. Zonulin, a regulator of epithelial and endothelial barrier functions, and its involvement in chronic inflammatory diseases. *Tissue Barriers* **2016**, *4*, e1251384. [[CrossRef](#)]
96. Bevivino, G.; Monteleone, G. Advances in understanding the role of cytokines in inflammatory bowel disease. *Expert Rev. Gastroenterol. Hepatol.* **2018**, *12*, 907–915. [[CrossRef](#)]
97. Guan, Q.; Zhang, J. Recent Advances: The Imbalance of Cytokines in the Pathogenesis of Inflammatory Bowel Disease. *Mediat. Inflamm.* **2017**, *2017*, 4810258. [[CrossRef](#)] [[PubMed](#)]
98. Nakase, H.; Sato, N.; Mizuno, N.; Ikawa, Y. The influence of cytokines on the complex pathology of ulcerative colitis. *Autoimmun. Rev.* **2022**, *21*, 103017. [[CrossRef](#)] [[PubMed](#)]
99. Neurath, M.F. Cytokines in inflammatory bowel disease. *Nat. Rev. Immunol.* **2014**, *14*, 329–342. [[CrossRef](#)]
100. Caviglia, G.P.; Ribaldone, D.G.; Nicolosi, A.; Pellicano, R. Cytokines and Biologic Therapy in Patients with Inflammatory Bowel Diseases. *Gastroenterol. Insights* **2021**, *12*, 443–445. [[CrossRef](#)]
101. Friedrich, M.; Pohin, M.; Powrie, F. Cytokine Networks in the Pathophysiology of Inflammatory Bowel Disease. *Immunity* **2019**, *50*, 992–1006. [[CrossRef](#)]
102. Berns, M.; Hommes, D.W. Anti-TNF-alpha therapies for the treatment of Crohn's disease: The past, present and future. *Expert Opin. Investig. Drugs* **2016**, *25*, 129–143. [[CrossRef](#)] [[PubMed](#)]
103. Ford, A.C.; Sandborn, W.J.; Khan, K.J.; Hanauer, S.B.; Talley, N.J.; Moayyedi, P. Efficacy of biological therapies in inflammatory bowel disease: Systematic review and meta-analysis. *Am. J. Gastroenterol.* **2011**, *106*, 644–659. [[CrossRef](#)] [[PubMed](#)]
104. Ungar, B.; Kopylov, U. Advances in the development of new biologics in inflammatory bowel disease. *Ann. Gastroenterol.* **2016**, *29*, 243–248. [[CrossRef](#)] [[PubMed](#)]
105. Bunte, K.; Beikler, T. Th17 Cells and the IL-23/IL-17 Axis in the Pathogenesis of Periodontitis and Immune-Mediated Inflammatory Diseases. *Int. J. Mol. Sci.* **2019**, *20*, 3394. [[CrossRef](#)] [[PubMed](#)]
106. Schmitt, H.; Neurath, M.F.; Atreya, R. Role of the IL23/IL17 Pathway in Crohn's Disease. *Front. Immunol.* **2021**, *12*, 622934. [[CrossRef](#)] [[PubMed](#)]
107. Noviello, D.; Mager, R.; Roda, G.; Borroni, R.G.; Fiorino, G.; Vetrano, S. The IL23-IL17 Immune Axis in the Treatment of Ulcerative Colitis: Successes, Defeats, and Ongoing Challenges. *Front. Immunol.* **2021**, *12*, 611256. [[CrossRef](#)]
108. Bosshart, H.; Heinzelmann, M. THP-1 cells as a model for human monocytes. *Ann. Transl. Med.* **2016**, *4*, 438. [[CrossRef](#)]

**Disclaimer/Publisher's Note:** The statements, opinions and data contained in all publications are solely those of the individual author(s) and contributor(s) and not of MDPI and/or the editor(s). MDPI and/or the editor(s) disclaim responsibility for any injury to people or property resulting from any ideas, methods, instructions or products referred to in the content.